

## Pt chemical species mapping in polymer electrolyte fuel cells by spatially-resolved nano-XAFS techniques

Polymer electrolyte fuel cells (PEFCs) are one of clean energy-converting devices with high power densities and efficiencies [1]. For widespread commercialization of PEFC vehicles, improvements in reliability and durability are indispensable. To solve these problems, testing and diagnostic methods, which can validate the membrane electrode assembly (MEA) catalyst designs and prove fundamental issues for development of next-generation PEFCs, are mandatory. Particularly, it is necessary to clarify key factors and mechanisms that promote or degrade performances of the Pt/C cathode catalyst and improve the durability for oxygen reduction reactions (ORRs). Key reaction processes, which regulate the durability of PEFCs as well as the ORR activity, may occur heterogeneously in the space of the cathode layer due to the following reasons: (1) the spatially heterogeneous property, (2) the distribution of Pt nanoparticles and carbon supports, and (3) the microscopically non-uniform potentials loaded in the cathode layer under the PEFC potential operations [2]. The cathode degradation mechanism has also been studied to improve the MEA durability, which is a serious issue. Therefore, the nanoscopic spatial place and mechanism of the dissolution and deterioration of the Pt/C cathode catalysts in MEAs should be elucidated to develop next-generation PEFCs with a high durability. Hence, we have investigated these properties at the new high-performance XAFS beamline BL36XU [3].

We prepared two types of MEAs as typical examples: (i) a MEA with a flat interface and few microcracks (denoted as MEA-A) and (ii) a MEA with microcracks (denoted as MEA-B) for nano-XAFS measurements. These MEAs were electrochemically aged and subjected an accelerated durability test (ADT). The treated MEAs were sliced into small pieces for nano-XAFS measurements under humid N<sub>2</sub> (Fig. 1). Because the samples are equivalent to MEAs *in situ* under the aging and ADT, the resultant nano-XAFS spectra are regarded as equivalent to the nano-XAFS spectra measured *in situ* after the aging and ADT cycles. We performed the scanning nano-XAFS mappings and nano-QXAFS measurements with nano-beams of 570 nm × 540 nm [4].

Figure 2 shows the scanning nano Pt L<sub>III</sub>-edge XANES mapping for MEA-A before (A and B) and after the ADT cycles (a and b). In the aged MEA-A, the Pt valence map (B) in the whole cathode area does not change significantly. The line profiles of the Pt quantity (blue) and Pt valence (red) along the red arrow of Fig. 2(B) are shown in Fig. 2(C). The Pt valence is metallic

in the whole region, while the distribution of Pt in MEA-A after the ADT cycles is heterogeneous (Fig. 2(a)). The line profiles of the Pt quantity (blue) and Pt valence (red) along the red arrow of Fig. 2(b) are shown in Fig. 2(c). It is noteworthy that the Pt valence in the cathode layer begins to increase at a distance roughly 3.2 μm away from the cathode layer edge and shows a maximum between the electrolyte and the Pt band (Fig. 2(d)). The oxidized Pt species produced initially at the boundary of the cathode catalyst layer during the operating process involving repeated potential loads.

Figure 3 exhibits the Pt L<sub>III</sub>-edge jump mapping (A) and Pt valence mapping (B) around the Pt/C cathode layer with a microcrack in MEA-B after the ADT cycles. The microcrack region shows much higher white line peak area (WLPA) values than the other cathode areas. It is noteworthy that the Pt valence in most parts of the microcrack region is calculated as 2+, whereas Pt nanoparticles in the other cathode areas are zero valent (metallic). In the microcrack region, Pt nanoparticles/nanoclusters are not observed by TEM, indicating that the microcrack region contains only sub-nanosized species and/or Pt ions. Figure 3(C) shows the nano-QEXAFS Fourier transforms (black), curve-fittings (red) and determined structural parameters for each area 1–6 in the microcrack region. Microcrack areas 1, 5, and 6 accommodate Pt<sup>2+</sup> species and the coordination numbers (CN) of Pt-O is 4.0 (±0.4) but Pt-Pt bonding is not observed. This means that the Pt<sup>2+</sup> species does not possess any Pt-Pt bonds but has a Pt<sup>2+</sup>-O<sub>4</sub> structure.

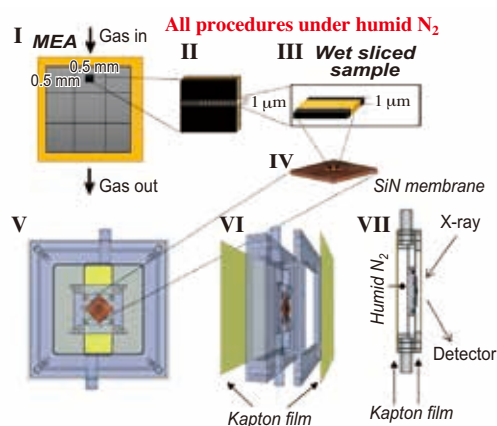


Fig. 1. Preparation and arrangement of a sliced MEA piece on a SiN membrane and its mounting in a XAFS cell for the nano-XAFS measurements. (I) Location of sample extraction, (II and III) dimensions for sample slicing, (IV) mounting on a SiN membrane, (V) front view of the designed cell, (VI) side view of stacked cells, and (VII) directions of the X-ray irradiation and XAFS detector.

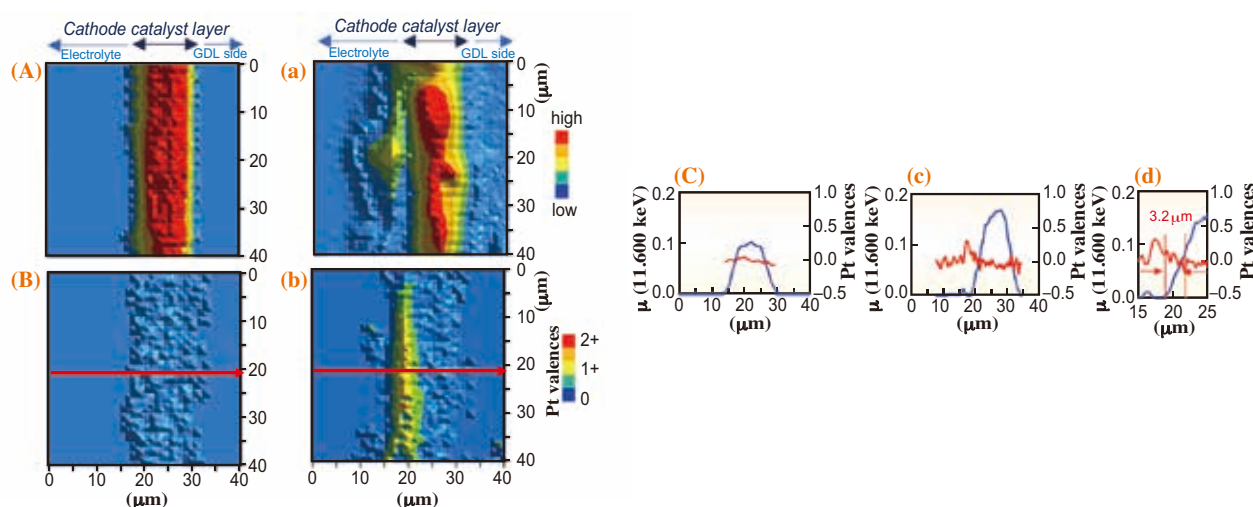


Fig. 2. (A and a) Pt  $L_{III}$ -edge jump mapping (Pt quantity mapping), (B and b) Pt valence mapping, for MEA-A after the aging (A, B) and ADT cycles (a, b) by the scanning nano (570 nm  $\times$  540 nm)-XAFS mapping method. (C and c) Line profiles of the absorbance ( $\mu$ ) at 11.600 keV (blue) and Pt valence (red) in the scanning nano-XANES spectra along the red arrows in B and b, respectively. (d) Enlarged line profile around the interface of the cathode catalyst layer and electrolyte.

In conclusion the present nano-XAFS study on the MEAs reports the first successful mapping of the Pt valence and identifies the major locations for oxidation and dissolution of Pt nanoparticles by the ADT cycles. The first spatial approaches to the Pt/C cathode catalysts in PEFCs by the scanning nano-XAFS mapping method and the nano-QXAFS method provide insight into the two-dimensional depth distribution of the metallic and

oxidized Pt species as well as the site-preferential mechanism for Pt oxidation and dissolution to form the  $Pt^{2+}$  monomeric species with a  $Pt-O_4$  coordination structure in the degradation process. *In situ* nano-XAFS experiments may provide a more in depth understanding of the MEA degradation mechanism by time-dependent mapping of the chemical change of Pt nanoparticles in PEFC MEA under various conditions.

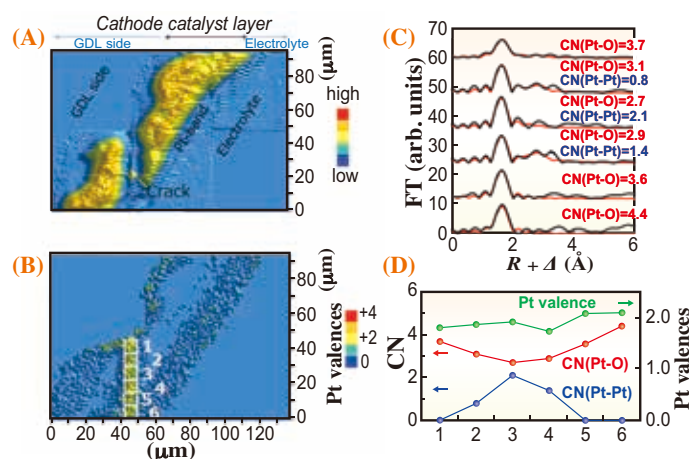


Fig. 3. (A) Pt  $L_{III}$ -edge jump mapping (Pt quantity mapping), (B) Pt valence mapping for MEA-B after the ADT cycles by the scanning nano-XAFS mapping method. (C) Nano-QEXAFS Fourier transforms (black) and curve-fittings (red) for microcrack areas (1-6) in B. (D) Nano QEXAFS analysis (CN(Pt-Pt):blue, CN(Pt-O):red) and Pt valence (green) for each microcrack area (1-6) in B.

Shinobu Takao\*, Oki Sekizawa and Yasuhiro Iwasawa

Innovation Research Center for Fuel Cells,  
The University of Electro-Communications

\*E-mail: takao@pc.uec.ac.jp

### References

- [1] G. Wu *et al.*: Science **332** (2011) 443; M.K. Debe: Nature **486** (2012) 43.
- [2] T. Saida *et al.*: Angew. Chem. Int. Ed. **51** (2012) 10311.
- [3] S. Takao, O. Sekizawa, S. Nagamatsu, T. Kaneko, T. Yamamoto, G. Samjeske, K. Higashi, K. Nagasawa, T. Tsuji, M. Suzuki, N. Kawamura, M. Mizumaki, T. Uruga, Y. Iwasawa: Angew. Chem. Int. Ed. **53** (2014) 14110.
- [4] O. Sekizawa *et al.*: J. Phys. Conf. Ser. **430** (2013) 012020.